Polymer 50 (2009) 5288–5292

Contents lists available at ScienceDirect

Polymer

journal homepage: www.elsevier.com/locate/polymer

Quantitative analysis of the cross-linked structure of microgels using fluorescent probes

Cathy Chu [a,b], Brian W. Schaefer [a], Ross J. DeVolder [a], Hyunjoon Kong [a,b,*]

[a] Department of Chemical and Biomolecular Engineering, University of Illinois at Urbana-Champaign, 114 Roger Adams Laboratory, 600 South Mathews Avenue, Urbana, IL 61801, USA
[b] Institute for Genomic Biology, University of Illinois at Urbana-Champaign, 1206 West Gregory Drive, Urbana, IL 61801, USA

ARTICLE INFO

Article history:
Received 20 July 2009
Received in revised form
28 August 2009
Accepted 6 September 2009
Available online 15 September 2009

Keywords:
Microgel
Liposome
Pyrene

ABSTRACT

Properties of polymeric microgels are influenced by the internal polymer cross-linked structure, but tools to quantitatively analyze this internal structure are limited. With the finding that polymer networks alter the diffusivity and subsequent excimer formation of pyrene, this study used the ratio between pyrene excimer and monomer emission to determine the number of cross-links (N) and average pore size (ξ) in poly(ethylene glycol) diacrylate (PEGDA) microgels. A calibration curve to relate pyrene emission to N and ξ in PEGDA hydrogels was prepared and used to calculate N and ξ in PEGDA microgels. The pyrene emission indicated that PEGDA microgels had a higher cross-linking density and a smaller average pore size when compared with bulk cross-linked hydrogels of the same PEGDA concentration. The analytical method demonstrated in this study may be useful for fine-tuning polymeric microgel properties for a broad array of applications.

1. Introduction

Polymeric microgels are used extensively in biological applications, such as drug delivery and cell encapsulation. The internal cross-linked structures of microgels regulate particle properties, including mechanical rigidity, structural stability, and porosity. In addition, the internal cross-linked structure affects the behavior of microgel particles, such as swelling [1,2], and the function of microgel particles, such as release rates of incorporated drugs or viability of encapsulated cells [3,4]. Despite effects of the internal structure on microgel properties, tools to analyze the microgel internal structure are limited. Properties of bulk cross-linked hydrogels are often used to predict microgel structure; however, due to differences between bulk polymerization and microgel polymerization [5,6], these methods are unable to precisely reflect the actual cross-linking density in microgels. Rheological measurements of microgel suspensions can be used to infer the relative cross-linking density within particles [7], but these measurements are also affected by interactions between particles. Swelling ratio measurements can be performed with microscopy and used to quantify the cross-linking density [8], but this technique becomes less useful as microgels become smaller. Ultimately, the development of a technique to directly probe and quantitatively analyze internal microgel structures could be useful for controlling the properties of microgel particles.

We hypothesized that water-soluble pyrene molecules could be used to quantitatively analyze the internal structure of microgels; such molecules have been previously used to probe the cross-linking density of polymeric hydrogels [9]. When excited at the appropriate absorption wavelength, individual pyrene molecules exhibit monomer emission profiles and stacked pyrene molecules exhibit excimer emission profiles. Excimer formation occurs when an excited pyrene molecule encounters a second pyrene molecule through diffusion [10]; the spatial organization of pyrene molecules is controlled by diffusion and depends on the surrounding microenvironment [11,12]. We propose that the cross-linked network influences the diffusivity and subsequent excimer formation of pyrene dissolved in microgels and that pyrene can thus be used to probe microgel structures. Our hypothesis was examined by analyzing the excimer and monomer emissions of pyrene molecules incorporated in liposome-templated and emulsion polymerized poly(ethylene glycol) diacrylate (PEGDA) microgels. The number of cross-links and average pore size of the microgels were calculated using calibration curves prepared from pyrene incorporated in bulk cross-linked PEGDA hydrogels. The internal cross-

* Corresponding author. Department of Chemical and Biomolecular Engineering, University of Illinois at Urbana-Champaign, 114 Roger Adams Laboratory, 600 South Mathews Avenue, Urbana, IL 61801, USA. Tel.: +1 217 333 1178; fax: +1 217 333 5052.
E-mail address: hjkong06@illinois.edu (H.J. Kong).

0032-3861/$ – see front matter © 2009 Elsevier Ltd. All rights reserved.
doi:10.1016/j.polymer.2009.09.019

linked structures were then compared with the theoretical cross-linked structures as predicted from bulk cross-linked hydrogels.

2. Experimental section

2.1. Preparation and pyrene analysis of bulk cross-linked PEGDA hydrogels

Poly(ethylene glycol) (MW = 508) diacrylate (PEGDA, Polysciences, Inc.) hydrogels were prepared from PEGDA solutions, varying from 15 to 100% (v/v), with potassium persulfate (KPS, Sigma Aldrich) and *N*,*N*,*N*′,*N*′-tetramethylethylenediamine (TEMED, Sigma Aldrich). Water-soluble 8-aminopyrene-1,3,6-trisulfonic acid, trisodium salt (pyrene trisulfonate, Invitrogen) was incorporated in the pre-gelled polymer solution, and the mixtures were allowed to gel between glass plates with a 1 mm spacer for 1 h at 37 °C. Hydrogel disks were punched and incubated in deionized water for 1 h. The fluorescent emission from 350 to 550 nm after excitation at 330 nm was collected with a fluorometer (Fluoromax-4, Horiba Jobin Yvon). The emission peak at 420 nm was regarded to represent the emission of monomers (I_{mo}), and the emission peak at 490 nm was regarded to represent the emission of excimers (I_{ex}). The area under the emission spectrum was integrated from 410 nm and 430 nm to quantify I_{mo} and integrated from 480 nm to 500 nm to quantify I_{ex}.

2.2. Quantification of cross-link number in bulk cross-linked PEGDA hydrogels

The compressive elastic moduli of the PEGDA hydrogel disks were measured using a mechanical tester (Insight, MTS Systems) by compressing the disks at a rate of 1 mm min^{-1}. The elastic moduli (E) of the disks were calculated from the linear slope of the stress (σ) versus strain (ε) curve for the first 10% strain. The shear moduli (G) were calculated from the linear slope of the stress versus $-(\upsilon - \upsilon^{-2})$ curve, where $\upsilon = 1 - \varepsilon$, for the first 10% strain. The degree of swelling (Q) of the gels were calculated as follows:

$$Q = \rho_p \frac{Q_m}{\rho_s} + \frac{1}{\rho_p} \tag{1}$$

where ρ_p represents the polymer density (1.12 g cm^{-3}), ρ_s represents the density of water, and Q_m represents the swelling ratio, which is defined as the mass ratio of hydrated disks to dry disks. The number of cross-links (N) within the gel disks was then calculated based on the rubber elasticity theory as follows [13]:

$$N = \frac{GQ^{1/3}}{RT} \tag{2}$$

where R represents the gas constant (8.314 J mol^{-1} K^{-1}) and T represents the temperature at which the modulus was measured (25 °C).

2.3. Quantification of pore size in bulk cross-linked PEGDA hydrogels

The average pore size (ξ) within the cross-linked networks was calculated from the following equation [14]:

$$\xi = \left(\nu_{2,s}^{-1/3}\right)\left(\overline{r_0^2}\right)^{1/2} \tag{3}$$

where $\nu_{2,s}$ represents the polymer volume fraction of the gel in the swollen state, which is equal to the inverse of the swelling ratio Q_m, and $(\overline{r_0^2})^{1/2}$ represents the unperturbed mean-square end-to-end distance of PEG. $(\overline{r_0^2})^{1/2}$ was calculated as follows:

$$\left(\overline{r_0^2}\right)^{1/2} = (l)(2nC)^{1/2} \tag{4}$$

where n represents the number of repeat units (=9), l represents the average monomer length (1.46 Å), and C represents the characteristic ratio for PEG (=4).

2.4. Preparation and analysis of liposome-templated PEGDA microgels

PEGDA microgels were prepared using liposome templates. Lipid layers were prepared by dissolving 1,2-dipalmitoyl-sn-glycero-3-phosphocholine (DPPC, Avanti Polar Lipids) in chloroform (Sigma Aldrich) and allowing the mixture to dry. The lipid layers were rehydrated with pre-gelled polymer solutions containing 5, 10, 20, and 50% (v/v) PEGDA along with the same concentrations of KPS, TEMED, and pyrene trisulfonate as used for the bulk cross-linked PEGDA hydrogel disks. Liposomes were formed by sonication with a sonic dismembrator (Fisher Scientific). To facilitate cross-linking exclusively within the liposomes, 4-methoxyphenol (Sigma Aldrich) was added to the sonicated mixture. 4-methoxyphenol inhibited cross-linking in the surrounding solution while the liposome interiors were allowed to gel for 1 h at 37 °C, resulting in cross-linked microgels with associated lipid layers. The microgel particles containing pyrene trisulfonate were separated from the surrounding free pyrene trisulfonate and resuspended in water; the fluorescent emissions from 350 to 550 nm after excitation at 330 nm were collected with a fluorometer.

To confirm the presence of cross-linked networks in PEGDA microgels, poly(ethylene glycol) methacrylate (Sigma Aldrich) was first labeled with rhodamine [15] and then incorporated in the pre-gelled polymer solution for microgel preparation. To confirm the presence of lipid membranes associated with PEGDA microgels, fluorescein octadecyl ester (Invitrogen) was used to stain the lipid layers prior to liposome formation. Particles were visualized with a Leica TCS SP2 laser scanning confocal microscopy system.

2.5. Preparation and analysis of emulsion polymerized PEGDA microgels

Pyrene analyses were also performed for PEGDA microgels prepared from emulsion polymerizations. The aqueous phase consisted of PEGDA solutions varying from 5 to 50% (v/v), polyvinyl alcohol (Sigma Aldrich), ammonium persulfate (APS, Sigma Aldrich), and pyrene trisulfonate. The organic phase consisted of dichloromethane (Sigma Aldrich) and TEMED. The aqueous phase and organic phase were mixed by vortex for 30 s and the resulting particles were allowed to gel at room temperature for 15 min. The particles containing pyrene trisulfonate were separated from the surrounding free pyrene trisulfonate and resuspended in water; the fluorescent emission from 350 to 550 nm after excitation at 330 nm was collected with a fluorometer. A corresponding calibration curve was prepared, as described above, from PEGDA hydrogel disks prepared with APS and TEMED.

3. Results

3.1. Calibration of pyrene emission with bulk cross-linked hydrogels

The first step to analyze microgel cross-linked structures involved calibrating the ratio of pyrene excimer and monomer emission intensities (I_{ex}/I_{mo}) to the number of cross-links (N) and the average pore size (ξ) of bulk cross-linked hydrogels. As the

PEGDA concentration was increased from 15 to 100%, the shear moduli increased from 90 to 2000 kPa while the swelling ratio decreased from 6.8 to 1.6 (SI, Fig. 1a). Accordingly, N calculated from the shear moduli and the swelling ratios [13] increased by an order of magnitude from 0.08 to 1×10^{-3} mol/cm^3 while ξ calculated from the polymer volume fraction and the unperturbed mean-square end-to-end distance of the monomer unit [14] decreased from 2.3 to 1.4 nm (SI, Fig. 1b). Pyrene analyses were performed in parallel by incorporating water-soluble pyrene trisulfonate in the PEGDA hydrogels. Excitation of pyrene trisulfonate from the polymer network at 330 nm resulted in an excimer emission peak at 490 nm and a monomer emission peak at 420 nm (SI, Fig. 2a). Excitation of pyrene trisulfonate dissolved in water resulted in an excimer emission peak at 490 nm (SI, Fig. 2b), while excitation of unmodified pyrene dispersed in water resulted in limited excimer emission (SI, Fig. 2c).

As the PEGDA concentration was increased from 15 to 100%, the ratio between the excimer emission intensity at 490 nm (I_{ex}) and monomer emission intensity at 420 nm (I_{mo}) decreased significantly (Fig. 1a). I_{ex}/I_{mo} was normalized with the PEGDA concentration to compensate for any effect the polymer concentration may have had on pyrene excimer formation. The normalized I_{ex}/I_{mo} decreased exponentially with increasing PEGDA concentrations (Fig. 1b). Plots relating the normalized I_{ex}/I_{mo} to $1/N$ (Fig. 1c) and ξ (Fig. 1d) were used as calibration curves to calculate N and ξ of PEGDA microgels.

3.2. Synthesis of liposome-templated PEGDA microgels

Microgels were prepared from the in situ polymerization of PEGDA solutions in the interior of liposomes. Lipid vesicles of 1,2-dipalmitoyl-sn-glycero-3-phosphocholine (DPPC) were first prepared with pre-gelled polymer solutions of PEGDA, initiator, and catalyst. The polymer solutions were then cross-linked in situ to form microgels with associated DPPC bilayers (Fig. 2a). As the PEGDA concentration was increased from 5 to 50%, the average microgel diameter decreased from 4.3 ± 1.9 to 1.0 ± 0.4 μm (SI, Fig. 3). The cross-linked microgel structure was confirmed with minimal changes in particle morphology after freeze-drying (SI, Fig. 4) and limited diffusion of incorporated rhodamine-conjugated poly(ethylene glycol) methacrylate molecules [15] (Fig. 2b; SI, Fig. 5). Lipid layers surrounding the particles were confirmed with the incorporation of fluorescein octadecyl ester in lipid films prior to microgel preparation (Fig. 2c).

3.3. Quantification of cross-link number and pore size in PEGDA microgels

The pyrene trisulfonate emission from microgels was then used to quantify N and ξ of PEGDA microgels. I_{ex}/I_{mo} decreased with increasing PEGDA concentration (Fig. 3), which agreed with the results from bulk cross-linked hydrogels. The I_{ex}/I_{mo} of microgel-free liposomes was similar to that of pyrene trisulfonate dissolved in water.

N and ξ of the microgels were then calculated from I_{ex}/I_{mo} values and the previously devised calibration curves (Fig. 1). As the PEGDA concentration in the microgels was increased from 5 to 50%, N increased from 0.05 to 1×10^{-3} mol/cm^3 (Fig. 4a) while ξ decreased from 2.5 to 1.5 nm (Fig. 4b). Interestingly, the cross-linking densities in 20 and 50% PEGDA microgels were higher than those in 20 and 50% PEGDA bulk cross-linked hydrogels, respectively, and the pore sizes were smaller in 20 and 50% PEGDA microgels than 20 and 50% PEGDA bulk cross-linked hydrogels, respectively.

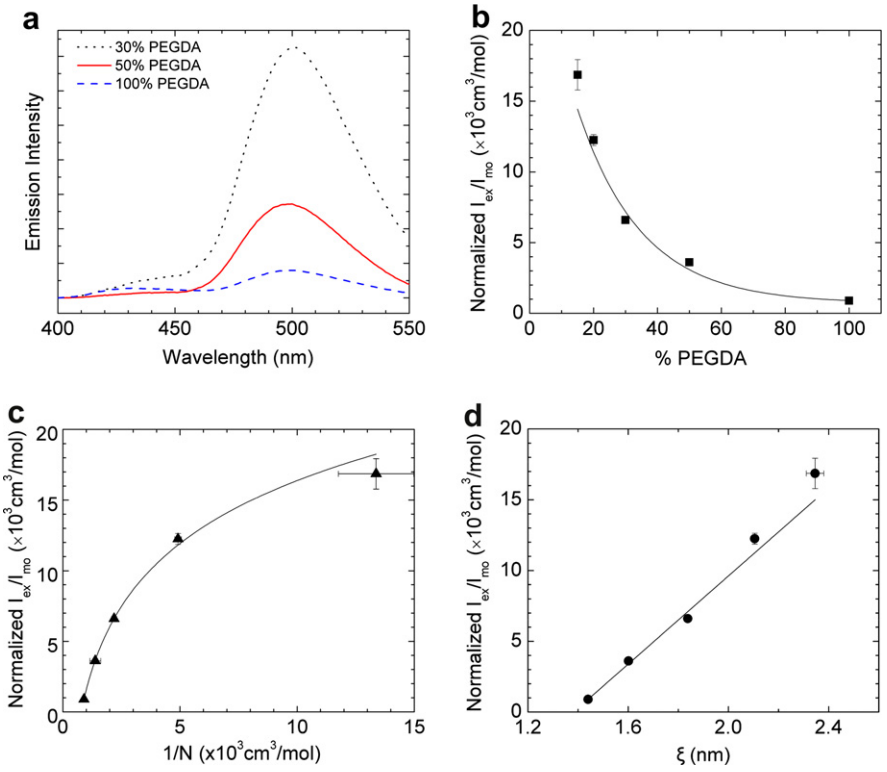

Fig. 1. Pyrene analyses for bulk cross-linked PEGDA hydrogels. (a) Pyrene excimer emission at 490 nm decreased with increasing PEGDA concentration, leading to (b) an exponential decrease in I_{ex}/I_{mo} with increasing PEGDA concentration. Calibration curves to relate (c) I_{ex}/I_{mo} to $1/N$ and (d) I_{ex}/I_{mo} to ξ were prepared from the pyrene analyses of bulk cross-linked PEGDA hydrogels.

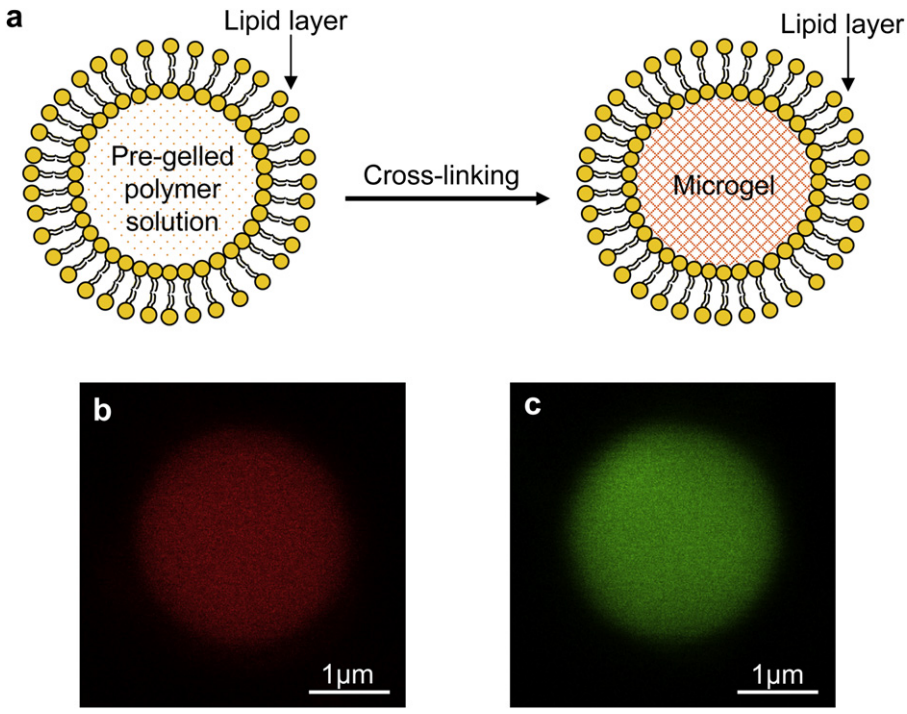

Fig. 2. Microgel particles. (a) Microgel particles were prepared by cross-linking polymer solutions of varied PEGDA concentrations in liposomes. This schematic description was confirmed with (b) red fluorescence from microgels containing rhodamine-conjugated poly(ethylene glycol methacrylate), and (c) green fluorescence from fluorescein octadecyl ester in lipid layers.

The N and ξ of PEGDA microgels prepared from emulsion polymerizations were also quantified with pyrene. First, calibration curves to relate I_{ex}/I_{mo} to $1/N$ (SI, Fig. 6a) and ξ (SI, Fig. 6b) were prepared from PEGDA disks produced with pyrene trisulfonate, APS, and TEMED, as described above. The emission from pyrene trisulfonate incorporated in emulsion polymerized microgels indicated a decrease in I_{ex}/I_{mo} with increasing PEGDA concentration, agreeing with the results from hydrogel disks and liposome-templated microgels. N (SI, Fig. 6c) and ξ (SI, Fig. 6d) of the emulsion polymerized microgels were calculated from I_{ex}/I_{mo} values and the corresponding calibration curves. The emulsion polymerized microgels had a higher cross-linking density and a smaller average pore size than corresponding bulk cross-linked hydrogels, agreeing with results from liposome-templated microgels.

4. Discussion

Altogether, the results of this study demonstrate a previously undescribed technique to quantitatively analyze microgel cross-linked structures using pyrene trisulfonate. First, the ratio between pyrene excimer and monomer emission intensities (I_{ex}/I_{mo}), as varied with the solids concentration in PEGDA hydrogels, was calibrated to the cross-link number and average pore size of the gels. Second, the pyrene emission was measured from PEGDA microgels, which were produced using liposome templates. I_{ex}/I_{mo} from microgels was then converted to cross-link number and average pore size using the calibration curves prepared from bulk cross-linked hydrogels. This technique was also used to quantify the cross-link number and average pore size of microgels prepared from emulsion polymerizations, indicating the versatility of this technique. Pyrene trisulfonate was used to probe the microgel structure because the solubility of these molecules in hydrophilic media allowed them to diffuse and rearrange in the hydrogel network. It has been well established that excimer formation is a diffusion-dependent process [11,12]. Since other factors which may affect excimer formation were constant in all experiments, we concluded that the excimer formation in this study was due to limited diffusion resulting from an increased number of cross-links

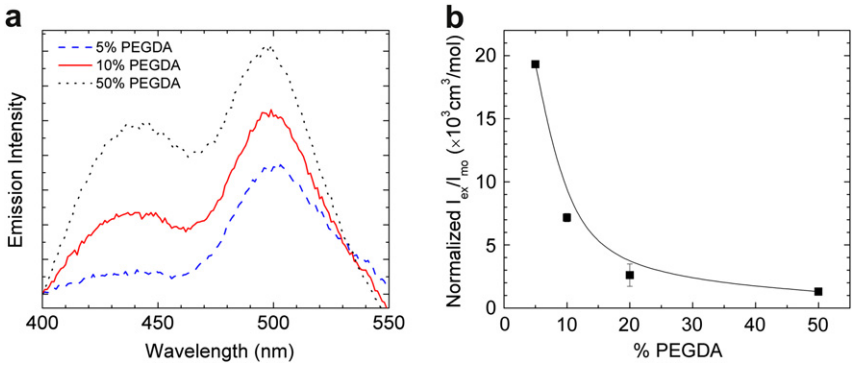

Fig. 3. Pyrene emission from PEGDA microgels. (a) As the PEGDA concentration increased, the pyrene monomer emission intensity at 420 nm increased more significantly than the excimer emission intensity at 490 nm, resulting in (b) a decrease of I_{ex}/I_{mo}.

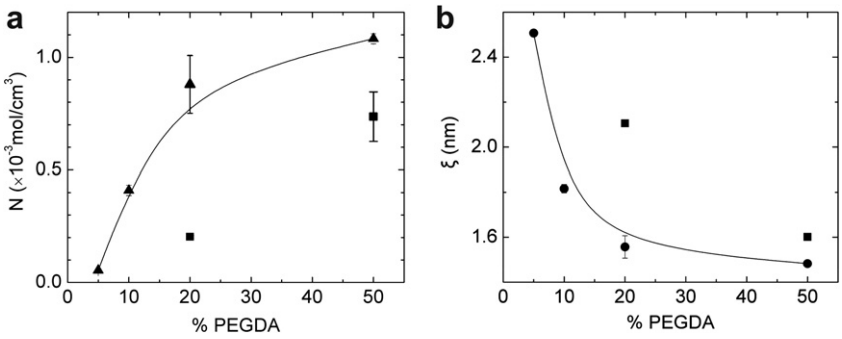

Fig. 4. The number of cross-links (N) and the average pore size (ξ) of PEGDA microgels were calculated using the pyrene emission from microgels and the calibration curve established with bulk cross-linked PEGDA hydrogels. (a) N in microgels (▲), as calculated with the calibration curve, increased with increasing PEGDA concentration. N in 20 and 50% PEGDA microgels were significantly higher than N in 20 and 50% PEGDA bulk cross-linked hydrogels (■), respectively. (b) ξ of microgels (●) decreased with increasing PEGDA concentration. ξ of 20 and 50% PEGDA microgels were smaller than ξ of 20 and 50% PEGDA bulk cross-linked hydrogels (■), respectively.

and decreased pore size. As the number of cross-links increased, the tendency of pyrene trisulfonate to form excimers decreased.

This pyrene-based assay indicated a higher cross-linking density and smaller average pore size in microgels when compared with bulk cross-linked hydrogels of the same chemical compositions. Such differences between microgel cross-linking and bulk cross-linking have been previously explained with kinetic modeling of emulsion polymerizations [5]. In addition, compartmentalization effects have been used to explain higher molecular weight distributions and tighter polymer networks in emulsion polymerizations compared with bulk polymerizations [16]. Discrepancies between the cross-linked structures of microgels and bulk hydrogels suggest that methods to directly examine interior microgel structures may be necessary.

Overall, this study demonstrates a novel method to analyze the internal structure of microgels using pyrene probes and also reveals structural differences between microgels and bulk hydrogels of the same chemical compositions. The pyrene-based assay described in this study may be useful for fine-tuning microgel structures synthesized from various methods [17] for a wide range of applications, such as drug delivery or cell encapsulation [18], and also allow one to non-invasively monitor microgel structural changes resulting from a variety of intrinsic and extrinsic factors [19–21].

Acknowledgements

The authors thank the American Heart Association (0830468Z) for financial support of this research. The authors also thank Dr. Jinwoong Kim of Amore Pacific Inc. for his invaluable comments.

Appendix. Supplementary data

The supplementary data associated with this article can be found in the on line version at doi:10.1016/j.polymer.2009.09.019.

References

[1] Eichenbaum GM, Kiser PF, Dobrynin AV, Simon SA, Needham D. Macromolecules 1999;32:4867–78.
[2] Senff H, Richtering W. Colloid and Polymer Science 2000;278:830–40.
[3] Langer R. Nature 1998;392:5–10.
[4] Schmidt JJ, Rowley J, Kong HJ. Journal of Biomedical Materials Research 2008;87A:1113–22.
[5] Tobita H. Macromolecules 1992;25:2671–8.
[6] Tobita H, Kumagai M, Aoyagi N. Polymer 2000;41:481–7.
[7] Hanyková L, Spěváček J, Ilavský M. Polymer 2001;42:8607–12.
[8] Kim JW, Larsen RJ, Weitz DA. Advanced Materials 2007;19:2005–9.
[9] Kong HJ, Lee KY, Mooney DJ. Macromolecules 2003;36:7887–90.
[10] Winnik FM. Chemical Reviews 1993;93:587–614.
[11] Birks JB, Dyson DJ, Munro IH. Proceedings of the Royal Society A 1963;275:575–88.
[12] Birks JB, Lumb MD, Munro IH. Proceedings of the Royal Society A 1964;280:289–97.
[13] Anseth KS, Bowman CN, Brannon-Peppas L. Biomaterials 1996;17:1647–57.
[14] Raeber GP, Lutolf MP, Hubbell JA. Biophysical Journal 2005;89:1374–88.
[15] Dalhaimer P, Engler AJ, Parthasarathy R, Discher DE. Biomacromolecules 2004;5:1714–9.
[16] Funke W, Okay O, Joos-Müller B. Advances in Polymer Science 1998;136:139–234.
[17] Utada AS, Lorenceau E, Link DR, Kaplan PD, Stone HA, Weitz DA. Science 2005;308:537–41.
[18] Das M, Zhang H, Kumacheva E. Annual Review of Materials Research 2006;36:117–42.
[19] Lowman AM, Morishita M, Kajita M, Nagai T, Peppas NA. Journal of Pharmaceutical Sciences 1999;88:933–7.
[20] Murthy N, Xu MC, Schuck S, Kunisawa J, Shastri N, Frechet JMJ. Proceedings of the National Academy of Sciences USA 2003;100:4995–5000.
[21] Ballauff M, Lu Y. Polymer 2007;48:1815–23.